EXPLORING ANTIFRAGILITY IN TRAFFIC NETWORKS: ANTICIPATING DISRUPTIONS WITH REINFORCEMENT LEARNING

Linghang Sun, Corresponding Author
Institute for Transport Planning and Systems
ETH Zurich, 8093 Zurich, Switzerland
Email: linghang.sun@ivt.baug.ethz.ch

Michail A. Makridis, Ph.D., Corresponding Author
Institute for Transport Planning and Systems
ETH Zurich, 8093 Zurich, Switzerland
Email: michail.makridis@ivt.baug.ethz.ch

Alexander Genser, Ph.D.
Institute for Transport Planning and Systems
ETH Zurich, 8093 Zurich, Switzerland
Email: alexander.genser@ivt.baug.ethz.ch

Cristian Axenie, Ph.D.
Computer Science Department
Technische Hochschule Nürnberg, 90489 Nürnberg, Germany
Email: cristian.axenie@th-nuernberg.de

Margherita Grossi, Ph.D.
Intelligent Cloud Technologies Lab
Huawei Munich Research Center, 80992 Munich, Germany
Email: margherita.grossi@huawei.com

Anastasios Kouvelas, Ph.D.
Institute for Transport Planning and Systems
ETH Zurich, 8093 Zurich, Switzerland
Email: kouvelas@ethz.ch

Word Count: 7923 words + 4 table(s) $\times$ 250 = 8923 words

Submission Date: October 11, 2023

ABSTRACT

The optimal operation of transportation networks is often susceptible to unexpected disruptions, such as traffic incidents and social events. Established control strategies rely on mathematical models that can not always deal with real-world uncertainty and their efficiency degrades remarkably under significant disruptions. While previous research works have dedicated efforts to enhancing the robustness or resilience of transportation systems against disruptions, in this paper, we use the concept of *antifragility* to better design a traffic control strategy for urban road networks. Antifragility sets itself apart from robustness and resilience as it represents a system's ability to not only withstand stressors, shocks, and volatility but also thrive and enhance performance in the presence of such disruptions. Hence, modern transport systems call for solutions that are more antifragile. In this work, we propose a model-free deep Reinforcement Learning (RL) algorithm to regulate perimeter control in a two-region urban traffic network to exploit and strengthen the learning capability of RL under disruptions and achieve antifragility. By incorporating antifragility attributes based on the change rate and curvature of traffic states into the RL framework, the proposed algorithm further gains knowledge on the change rate of the traffic state, which helps with anticipating imminent disruptions. An additional dynamic redundancy term is also integrated into the RL algorithm to enhance the performance of the traffic control strategy under disruption scenarios. We present the proposed RL algorithm as being antifragile in comparison to a model-based control-theory method and a state-of-the-art RL algorithm, showcasing its ability to learn from past events and outperform the other methods, particularly under increasing disruptions.

Keywords: Antifragility, Reinforcement Learning (RL), Traffic disruptions, Perimeter control, Macroscopic Fundamental Diagram (MFD).

INTRODUCTION

Transportation networks serve as vital conduits for the movement of people and goods. The optimization of these transportation systems has become a focal point for transportation researchers, resulting in a multitude of research endeavors and practical implementations in the field of Intelligent Transportation Systems (ITS), as in (*1–3*). Given that various sorts of incidents, such as traffic accidents, social events, unfavorable weather conditions, etc., often occur unexpectedly in real-world networks, examining the robustness and resilience of the transportation system's performance to handle disturbances and disruptions is crucial in the research of ITS (*4*).

With the ever-growing population in the cities and urbanization, traffic systems have gained both volume and complexity. For instance, according to the Federal Statistical Office of Switzerland, private motorized road traffic experienced a steady increase of 54% in total between 1980 and 2019 (*5*). Also, as pointed out in (*6*), the rise in traffic volume can result in an escalation of intensified congestion and more traffic incidents. Therefore, new requirements have been constantly posed to the urban road networks, to secure a decent level of service even when confronted by various disruptions with unforeseen magnitude. This also raises the question of whether the current levels of robustness and resilience in transportation systems are sufficient to handle such challenges.

To address such issues, "antifragility" has shed light on a feasible solution and provides a possible new evaluation criterium. The concept of antifragility, first introduced in the bestseller *Antifragile: Things that Gain from Disorder* by Nassim Nicholas Taleb in 2012 and mathematically explained in (*7*) and (*8*), provides insights on designing systems that can benefit from disruptions and perform better under growing disorder. Since then, antifragility has gained great interest from both the public and also academia, particularly in the field of risk engineering (*9*). The potential of antifragility can also be leveraged within transportation systems to tackle the increasingly severe traffic problems modern cities face from day to day.

However, how to identify and even design antifragile transportation systems remains unstudied. One promising approach to induce antifragility in urban road networks is by using learning-based algorithms. With the rapid advancement of big data and sensor techniques, using Machine Learning (ML), particularly Reinforcement Learning (RL)-based methods has also become a trending practice in designing traffic management and control strategies in ITS (*10–12*). Through interacting with a given environment over time, an RL agent enhances its decision-making ability, maximizing the cumulative reward it can receive (*13*). One advantage of RL over established controllers is that it allows for more flexibility and competence to deal with multivariate nonlinearities in complex environments (*14, 15*). When deployed to an environment subject to variations, RL agents can gradually adjust their decision-making by interacting with the new environment, whereas established controllers, such as PID controllers, may need intensive manual tuning of parameters (*16*). Also, additional information can be fed to the RL agent with ease as a representation of the observable state of the environment, regardless of the knowledge of the model dynamics. In contrast, structured model dynamics of the system are often required when designing a controller (*17*). This feature of RL can also be exploited to explore hidden information from the abundance of data in the field of transportation, and modern traffic control systems can potentially learn from traffic disruptions, react proactively with merely early signs, and exhibit increasingly better performance as disruptions escalate.

The main goal of this paper is to first distinguish the concept of antifragility as opposed to other more commonly used terms, i.e., robustness and resilience, under the context of trans-

portation. Then we demonstrate how an antifragile RL algorithm can be designed to empower traffic control strategies, such as perimeter control in this study, to be antifragile against disruptions with various magnitudes. We also propose a quantitative approach to evaluate and compare the antifragility property among different methods.

LITERATURE REVIEW

This section provides a review of the relevant literature with three topics covered in this work. First, a macroscopic traffic model and the control strategy applied in this paper are introduced, which serve as the basis of model dynamics for our simulation environment. Following that, since antifragility itself is a relatively new topic and the link between RL and antifragility is yet absent, we present state-of-the-art research on leveraging RL algorithms to enhance the robustness and resilience of control strategies. Finally, based on the literature, we introduce antifragility conceptually and how an antifragile system can be designed.

Alleviating urban network congestion can be realized through various traffic control strategies. One common practice of achieving less congested networks is through traffic signal control. This microscopic control approach on an intersection level can be extended to a corridor or a larger urban network with proper coordination. However, fine-grid coordinated microscopic signal control can be computationally demanding to be implemented in real-time on a large-scale urban network (*18*). Since (*19*) proved the existence of the Macroscopic Fundamental Diagram (MFD) theoretically and (*20*) demonstrated the presence of the MFD with empirical data, the relationship between average traffic flow and density has been established through the aggregation of individual microscopic data points. This relationship has paved the way for the development of control strategies on a macroscopic level, enabling more computationally feasible real-time control strategies for large-scale networks (*21*). With the MFD and the identification of the critical parameters, several control methods have been proposed to enhance the performance of road networks, such as perimeter control (*22–24*), pricing (*25–27*) and route guidance (*28–30*).

Perimeter control is among the methods that have attracted immense attention and research. Real-world implementation as shown in (*31*) also demonstrated the applicability of perimeter control as an effective approach to regulating urban traffic. By refraining the incoming vehicles from adjacent regions into a protected zone, the traffic density in the protected area remains below the critical density, so a satisfactory level of service can be upheld (*32*). (*22*) proposed an optimal perimeter control method using Model Predictive Control (MPC) and proved its effectiveness compared to a greedy controller in a cordon-shaped network. However, within the context of this paper, the problem with MPC is that it necessitates an abundance of a priori knowledge (*33*), which may not be readily available in real-world applications and is hard to forecast with high fidelity. Also, since disruptions, such as traffic accidents, can neither be known nor accurately predicted in advance, the performance will be negatively affected when large disruptions would happen in real-world networks. Another problem with the previous works is the MFD heterogeneity and uncertainty. To address the heterogeneity of the MFDs in different sub-regions, a substantial amount of effort has been made in investigating the partitioning algorithms so that a well-defined MFD can be referred to for a certain sub-network (*34, 35*). Following the partitioning, the cordon network has been expanded into multi-reservoir systems and these works implemented perimeter control based on methods either without coordination (*36*) or with coordination (*37*). (*23*) combined a model-based perimeter control design with an online adaptive fine-tuning algorithm. Although these studies are based on the assumption of static well-defined MFDs, in reality,

MFDs can hardly be always well-defined, as shown in (*38*) with loop detector data over a year. Research works based on real-world data have demonstrated that certain types of disruptions, such as adverse weather conditions (*39*) and traffic incidents (*40*), can alter the shape of the MFDs and even a recovery from the peak-hour congestion may lead to a hysteresis (*41*). These phenomena could potentially violate the mathematical model that serves as the foundation for the established model-based perimeter controllers. Also, increasing model errors and disturbances will cause the effectiveness of these control strategies to decline progressively (*42*).

To tackle the parameter uncertainties in the models caused by real-world disruptions, recent years have also witnessed a growing trend towards utilizing non-parametric learning-based approaches in traffic control (*43*), owing to the abundance of data collected from multiple sources such as loop detectors, video cameras, and mobile networks. Among different ML algorithms, RL has been researched extensively in transportation operations, e.g., traffic light control (*44, 45*), dynamic pricing (*46, 47*), delay management (*48, 49*). Particularly for perimeter control, recent works from (*50*) and (*51*) have illustrated the capability of RL algorithms to achieve comparable or even better performance in perimeter control compared to the established control methods.

Before introducing the concept of antifragility, two related terms *robustness* and *resilience* commonly used to evaluate traffic control strategies are compared here. As stated in (*52*), the concepts of robustness and resilience vary significantly according to their usage in different disciplines. Also, (*53, 54*) mentioned that these terms are sometimes used interchangeably in transportation research works. While researchers have endeavored to produce review articles in either the applications of RL in transportation (*12, 55*) or robustness/resilience in transportation systems (*56, 57*), a summarization of using RL algorithms in transportation to achieve robust or resilient urban networks remains absent. Here we made a brief review of the established works using RL to regulate urban traffic, either microscopically or macroscopically, that touched upon proving the robustness or resilience of their proposed methods. By transferring the knowledge of robust or resilient design, we can achieve antifragility in urban networks through similar approaches. Table 1 shows a selection of papers around perimeter control and traffic signal control designed with RL algorithms. The objectives, the application scenarios, and the property of being either robust or resilient, as claimed by the authors, are also listed in the table.

As can be seen, 2 out of the 10 reviewed papers are focused on the resilience of the RL-based traffic control strategies and the studied scenarios are traffic demand uncertainties and MFD errors (*60*) as well as lane closures (*66*). When examining the system's robustness, the types of scenarios under consideration become more diverse, including incidents (*61, 63*), sensor failures (*65*), other than varying demand patterns. However, as mentioned above, the common interchangeable usage of robustness and resilience makes it challenging to establish a definitive differentiation between robustness and resilience based on their application scenarios. Therefore, we follow the principles proposed by (*56*), that robustness is concerned with assessing a system's capacity to preserve its initial state and resist performance deterioration in the presence of uncertainty and disturbances, while resilience stresses the capability and speed of a system to recover from disruptions to the original state, as in the lane closure scenario in (*66*). Since maintaining the original state is difficult for systems when confronted with significant disruptions, such events are usually associated with the study of resilience (*67*).

Table 2 summarizes the RL setups to demonstrate the property of being either robust or resilient of each traffic control strategy. In these papers, some authors proved the superior robustness or resilience of their proposed methods directly through testing against the established methods as

TABLE 1: Traffic Control Strategies Using RL with Demonstrated Robustness or Resilience

Literature	Category	Objective	Scenarios	Robust	Resilient
(*51*)	Perimeter control	Maximize trip completion under uncertainties	Demand and MFD uncertainties	×	
(*58*)	Perimeter control	Minimize total time spent under uncertainties/disturbances	Demand uncertainties, demand surge	×	
(*59*)	Perimeter control	Maximize trip completion under uncertainties	Demand uncertainties	×	
(*60*)	Perimeter control	Maximize trip completion under uncertainties and errors	Demand and MFD uncertainties		×
(*61*)	Traffic signal control	Minimize average travel time under disturbances	Incidents, sensor noise	×	
(*62*)	Traffic signal control	Minimize queue length and delay, maximize vehicle speed and trip completion under demand uncertainties	Demand uncertainties, demand surge	×	
(*63*)	Traffic signal control	Minimize total travel time, total delay, and total stop time	Demand surges, incidents, sensor failures	×	
(*64*)	Traffic signal control	Minimize queue length at the intersection under uncertainties	Demand uncertainties	×	
(*65*)	Traffic signal control	Minimize average vehicle delay under different scenarios	Demand uncertainties, sensor noise	×	
(*66*)	Traffic signal control	Minimize average travel time under disruptions	Lane closure		×

benchmarks, whereas others induced such properties by adding specific terms (italicized in Table 2) in the state space of the RL-algorithm. As a result, the algorithms are given additional information, which potentially empowers the algorithms to anticipate ongoing disruptions. For instance, (*63*) induced robustness by adding the elapsed time since the last green signal for each phase, (*64*) experimented with speed or pressure (residual queue) as an additional state representation in the state space of the RL algorithm, (*62*) supplemented the control policies of neighboring intersec-

TABLE 2: RL Setups for Studying Robustness or Resilience in Traffic Control

Literature	Robustness	Resilience	Benchmark	RL method	State	Action	Reward
(*51*)	Tested[1]		No-control, MPC	DDPG	Number vehicles, traffic demand	Perimeter control variables	Trip completion
(*58*)	Tested		MPC	AC-IRL	Number vehicles	Perimeter control variables	Divergence from critical accumulation
(*59*)	Tested		FT/Webster/ MP + PI	DQN	Flow, density, speed	Perimeter control variables	Ratio of flow over max flow
(*60*)		Induced[1]	No-control, MPC	MADDPG	Number vehicles, traffic demand, *congestion indicator*[2]	Perimeter control variables	Trip completion
(*61*)	Tested		Cross comparison	DQN, AC, SARSA	Phase, pressure	Green time duration	Queue length
(*62*)	Induced		IA2C, IQL-LR, IQL-DNN	MAA2C	Total delay, number vehicles, *adjacent info*	Signal configuration	Queue length, total delay
(*63*)	Induced		Self-comparison	DDQN	Queue length, *elapsed time in each phase*	Time extension, phase selection	Numerical derivative of queue length
(*64*)	Induced		Self-comparison	DDQN	phase info, queue length, *speed, pressure*	Phase configuration	Queue length, duration over detection
(*65*)	Tested		Fixed-time, actuated	DDQN	Phase, number vehicles, elapsed time, neighbour phases	No-change/ extend/ terminate	Queue length
(*66*)		Tested	Random, cyclical, demand, analytical+	DQN, DQN + heuristic	Vehicle occupancies	Green time duration	Negative pressure

[1] Tested/Induced means whether the property of robustness or resilience is demonstrated through testing against other benchmark methods or the author claimed to have implemented specific methods to induce the robustness or resilience of the proposed method.

[2] Italicized terms represent the additional information the authors applied and claimed as effective to design a robust/resilient system.

tions as additional information to the agents, and (*60*) used an extra binary congestion indicator in the state space. These works demonstrated better performance of the proposed algorithms in comparison with established methods or through self-comparison.

Ever since the concept of antifragility has been proposed, it has become an increasingly

popular concept in many disciplines, such as economy (*68*), business (*69*), biology (*70*), medicine (*71*), and robotics (*72*). However, current studies on antifragility in the field of engineering mostly pertain to post-disaster reconstruction efforts (*73–75*). Leveraging the potential of antifragility for the daily operations and optimization of transportation systems is a new and unexplored notion.

Although not explicitly stated in the book or in any scientific paper, researchers' understanding of antifragility is two-fold. The first understanding resembles adaptiveness. A robust system tends to maintain its original state amidst model and input uncertainties, resilience enables a system to recover from disruptions within a period of time. In contrast, antifragile systems aim to enhance performance in a progression of unexpected events, such as in (*73*). These events are often referred to as black swan events (*76*), suggesting that the magnitude of disruptions is unexperienced and likely to exceed the capacity of system robustness to manage. Another understanding, which may be less intuitive but can be grasped by considering its antonym, i.e., fragility, refers to an object or a system that suffers from exponentially growing loss when faced with linearly increasing disruptions (*8*). This concept is characterized by concavity and can be mathematically formulated with Jensen's inequality $E[g(X)] \leq g(E[X])$. On the contrary, the nonlinear relationship between external stressors and responses for antifragile systems is convex with $E[g(X)] \geq g(E[X])$. Since the difference is not clearly distinguished, in our work, we will refer to the different understandings as antifragility type I (adaptiveness) and antifragility type II (concavity).

Researchers have also proposed methods to incentive antifragility property of a system by emphasizing the derivatives to capture the temporal evolution patterns of the system dynamics, i.e., how fast the system state deviates towards a possible black swan event, and the curvature of this deviation (*8, 71, 77*). With this additional information, the system can anticipate ongoing disruptions and be more responsive to drastic changes. Similar to the function of redundancy in resilience (*78, 79*), another feasible approach to induce system antifragility is to add redundancy in the system (*76, 80, 81*).

In this work, we simulate a cordon-shaped urban road network, subject to demand disruptions. Rather than relying on a mathematical model and static traffic indicators to determine the best policies for perimeter control, we use a model-free RL-based approach that adopts the concept of antifragility. To achieve this, we integrate supplementary state and reward components derived from derivatives and redundancy into the RL algorithm. This integration allows the algorithm to exhibit the characteristic to acquire knowledge from previous disruptions and become antifragile. The key contributions of this work can be summarized as follows: This work is the first to embrace the concept of antifragility in the context of the daily operation of transportation systems. The study demonstrates the effectiveness of incorporating derivatives and redundancy to handle system disruptions. Also, the proposed antifragile model-free RL-based algorithm achieves better performance compared to both a model-based control strategy that requires a priori knowledge and the other state-of-the-art model-free RL-based methods.

To enhance the clarity of the paper's structure, the study will proceed as follows: Section 6 formulates mathematically the cordon network and the model dynamics of perimeter control, and summarizes all the applied notations in this paper. Section 5 explains the applied control methods MPC and RL-based algorithms in detail and describes specifically the mathematical definition of antifragility, and how we can induce antifragility in a transportation system. Section 6 introduces the specifications of the tested environment and the evaluation metrics, while Section 7 presents the results to showcase the effectiveness and antifragility of our proposed method.

PROBLEM FORMULATION

This paper studies the problem of perimeter control between two homogeneous regions. A cordon-shaped urban network is investigated as in (*22, 51*), with the inner region representing a city center, as shown in Figure 1a, and traffic demand for an Origin-Destination (OD) pair from region i to region j at time t is denoted as $q_{ij}(t)$. The inner and outer regions have different MFDs due to the difference in capacity to accommodate vehicles in the road networks within the city center and the surrounding region, defined as $G_i(n_i(t))$ as illustrated in Figure 1b. Given the total number of vehicles, denoted as $n_i(t)$ with presence in region i at time t, the total trip completion rate, denoted as $M_i(t)$ for this region i can be determined using the corresponding MFD, which comprises both the intraregional trip completion, i.e., $M_{ii}(t)$ and the interregional transfer flow, i.e., $M_{ij}(t)$ $(i \neq j)$ with $i, j \in \{1,2\}$. In order to protect both regions from being overflown by possible high traffic demand, the percentage of the transfer flow allowed to go across the region perimeter at time t is regulated by two perimeter controllers denoted as $u_{ij}(t)$ $(i \neq j)$. A list of all notations used in this paper, including the notations used in defining the RL algorithm and the antifragile terms, is summarized in Table 3.

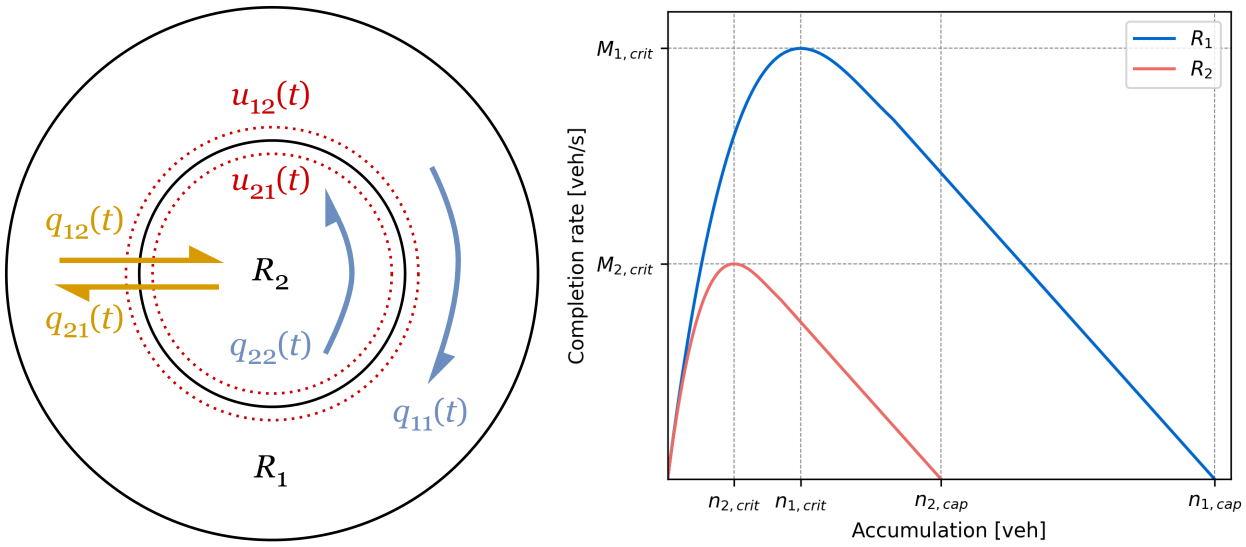

(a) The cordon-shaped urban network

(b) MFDs for the inner and outer regions

FIGURE 1: The network structure and the related MFDs

Eq. 1 describes the change rate of the vehicle accumulation within a specific region i and is the sum of intraregional traffic demand together with the perimeter control regulated transfer flow from region j deducted by the trip completion within region i. The change rate of interregional traffic accumulation, as in Eq. 2 shows, is the difference between the interregional traffic demand and the regulated transfer flow:

$$\frac{dn_{ii}(t)}{dt} = q_{ii}(t) + u_{ji}(t) \cdot M_{ji}(t) - M_{ii}(t) \tag{1}$$

$$\frac{dn_{ij}(t)}{dt} = q_{ij}(t) - u_{ij}(t) \cdot M_{ij}(t), \ (i \neq j) \tag{2}$$

The total trip completion, i.e., $M_i(t)$ for region i at time t is calculated based on the trip

TABLE 3: List of Notations

Symbol	Meaning
1. General notations in problem formulation	
t	Time
Δt	Time step
t_{end}	Total simulation time
$n_{ij}(t)$	Vehicle accumulation with OD from region i to j at time t
$n_i(t)$	Vehicle accumulation in region i at time t
$u_{ij}(t)$	Perimeter control variables regulating flow from region i to j at time t
$q_{ij}(t)$	Traffic demand with OD pair i and j at time t
$G_i(n_i(t))$	Sum of trip completion and transfer flow in region i at time t, equals to $M_i(t)$
$M_{ij}(t)$	Trip completion rate with OD from region i to j at time t
$n_{i,cap}(t)$	Maximal possible number of vehicles (jam accumulation) in region i at time t
$n_{i,crit}(t)$	Critical number of vehicles with highest completion rate in region i at time t
J	Objective function
2. Notations in reinforcement learning	
$\mathscr{S}$	State space, the whole set of states the RL agent can transition to
s_t	$s_t \in \mathscr{S}$, the observable state in simulation at time t
$\mathscr{A}$	Action space, the whole set of actions the RL agent can act out
a_t	$a_t \in \mathscr{A}$, the action taken in simulation at time t
$\mathscr{R}$	The reward function for the RL agent
r_t	$r_t = \mathscr{R}(s_t, a_t)$, the received reward in simulation at time t
γ	Discount factor to favor rewards in the near future
$Q(s(t), a(t))$	Expected long-term return for taking action $a(t)$ in state $s(t)$ at time t
θ^{μ}	Weight of the deep neural network for the actor network
θ^{Q}	Weight of the deep neural network for the critic network
y_i	Expected long-term return calculated with the target critic network
L	The loss of the critic network
ρ^{β}	All possible trajectories of s_t
I	The objective function for the actor network
3. Notations for the additional antifragile terms applied in reinforcement learning	
$\varepsilon(t)$	Additional reward term in RL based on derivatives and redundancy
ω_h	The weight of first derivative in the additional reward term $\varepsilon(t)$
$\omega_{\Delta h}$	The weight of second derivative in the additional reward term $\varepsilon(t)$
$\alpha_i(t)$	Binary variable determining the term to be reward/penalty
$h_i(t)$	The first derivative of traffic state at time t
$\Delta h_i(t)$	The second derivative of traffic state at time t

accumulation, denoted by $n_i(t)$ through MFD, defined as $G_i(n_i(t))$ and consists of two parts, intraregional trip completion, i.e., $M_{ii}(t)$, in Eq. 3 and interregional transfer flow, i.e., $M_{ij}(t)\,(i \neq j)$, in Eq. 4:

$$M_{ii}(t) = \frac{n_{ii}(t)}{n_i(t)} \cdot G_i(n_i(t)) \tag{3}$$

$$M_{ij}(t) = \frac{n_{ij}(t)}{n_i(t)} \cdot G_i(n_i(t)),\ (i \neq j) \tag{4}$$

$$n_i(t) = \sum_{j=1,2} n_{ij}(t) \tag{5}$$

The objective function is to maximize the throughput of this corden-shaped network, which is the sum of the intraregional trip completion, which is $M_{ii}(t)$ in both regions.

$$J = \max_{u_{ij}(t)} \int_0^{t_{end}} \sum_{i=1,2} M_{ii}(t)dt \tag{6}$$

subject to the following boundary conditions:

$$n_{ij}(t) \geq 0 \tag{7}$$

$$n_i(t) \leq n_{i,cap} \tag{8}$$

$$u_{min} \leq u_{ij}(t) \leq u_{max} \tag{9}$$

$n_{ii}(t)$ and $n_{ij}(t)$ are intraregional and interregional vehicle accumulation and are non-negative values. $n_{i,cap}$ is the maximal possible number of vehicles accumulated in region i, which can lead to a gridlock as shown in Figure 1b. u_{min} and u_{max} represent the lower and upper limit for the perimeter control variable $u_{ij}(t)$ for both directions and such applications are in line with (*22, 51*). These bounds are due to the fact that perimeter control is normally implemented through signalization. While u_{max} accounts for the lost time caused by the interchange between the red and green phases, u_{min} describes that complete perimeter control through an indefinite long red light is rare in real-world cases.

In contrast to the control-based strategies, for the RL-based algorithms, following the idea of redundancy, an additional term $\varepsilon(t)$ is added into the objective function J_{RL}, referred to as reward $r_t \in \mathscr{R}$ under the context of RL, leading to:

$$J_{RL} = \max_{u_{ij}(t)} \int_0^{t_{end}} [\sum_{i=1,2} M_{ii}(t) + \varepsilon(t)]dt \tag{10}$$

The term $\varepsilon(t)$ aims to build up a proper redundancy so that the proposed RL algorithm does not reward the agent for targeting the exact critical accumulation point. A comprehensive explanation of the term $\varepsilon(t)$ for the reward in RL will be provided in the following Section 5.3.

METHODOLOGY

This section gives a brief explanation of how MPC and RL are applied in this paper, and how we realize designing an antifragility perimeter control strategy based on the derivatives and redundancy in detail.

MPC algorithm

MPC is an established control method with wide applications in engineering to regulate dynamic systems (*82*), and is used as one of the benchmark methods in this work. First applied in (*22*), MPC has been proven to be an effective and robust method to regulate perimeter control in comparison to a greedy controller under both normal situations and traffic demand uncertainties as well as MFD errors. For details of the implementation of MPC in general practice or under the context of perimeter control, we refer the readers to (*83*) and (*22*). The applied MPC toolkit in this paper is introduced in (*84*), which uses the CasADi framework (*85*) and the NLP solver IPOPT (*86*).

The disadvantage of MPC is that it assumes an abundance of a priori knowledge, which includes traffic demand at each time step, but this information is hardly available in real-world applications. Although traffic forecasting (*87, 88*) may serve as a substitute for real traffic demand, the prediction accuracy is not always guaranteed. Potentially the information on disruptions, such as the distribution of the surging demand, can also be fed into MPC so that the algorithm can yield more accurate results. However, it is self-evident that disruptions are mostly fully unexpected events without any a priori knowledge. Therefore, in our research, when disruption takes place in the simulation, we apply the same control policies generated by MPC under an aggregated scenario. This aggregated scenario is the weighted average of the past traffic demand profiles, which includes all the experienced disruptions except the current one.

RL algorithm

A perimeter control strategy using RL has been proven feasible in (*50, 51, 58*), In RL algorithms, an agent or multiple agents interact with a preset environment and improve the performance of decision-making, defined as action a_t in an action space $\mathscr{A}$, based on the observable state s_t in the state space $\mathscr{S}$ and the reward, defined as $r_t = \mathscr{R}(s_t, a_t)$, where $\mathscr{R}$ is the reward function. The improvement of decision-making is commonly realized through a deep neural network as a function approximator. The RL algorithm applied in this work is Deep Deterministic Policy Gradient (DDPG) as proposed in (*89*). By applying an actor-critic scheme, DDPG can manage a continuous action space, i.e., allowing the perimeter control variables to be continuous instead of only choosing from a limited set of discrete values. In contrast, the traditional Deep Q-Network (DQN) algorithm (*90*) commonly applied as in Table 2 shows, can only be applied in an environment with a discrete action space. Even though a discrete action space is also viable to determine the change rate of the perimeter variables, (*51*) has proven that an RL algorithm with continuous action space can achieve better performance compared to discrete action space. The DDPG algorithm can be divided into two main components, namely the actor and the critic, which are updated at each step through policy gradient and Q-value, respectively. The scheme of the DDPG algorithm applied in this paper is schematically illustrated in Figure 2.

The state $s_t \in \mathscr{S}$ is defined distinctively according to different methods applied in this work. Our proposed method consists of three terms, the vehicle accumulation regarding the OD pair $n_{ij}(t)$, the change rate of vehicle accumulation at each time step $dn_{ij}(t)$ (first derivative) as well as the second derivative $d^2n_{ij,t}$. In (*51*), a state s_t defined as $[n_{ij}(t), q_{ij}(t)]$ is adopted. However, since traffic demand in the real world is hardly measurable, meaning $q_{ij}(t)$ should be an unobservable state for the agent. In our work, only variables that are observable or deducible for the agents can be incorporated, which are $n_{ij}(t)$, $dn_{ij}(t)$, and $d^2n_{ij}(t)$ in our case. The action $a_t \in \mathscr{A}$ is defined the same as the control variables $u_{ij}(t)$. The reward for our proposed method is defined as in Eq. 10 describes while the baseline method uses only the completion rate as the reward term.

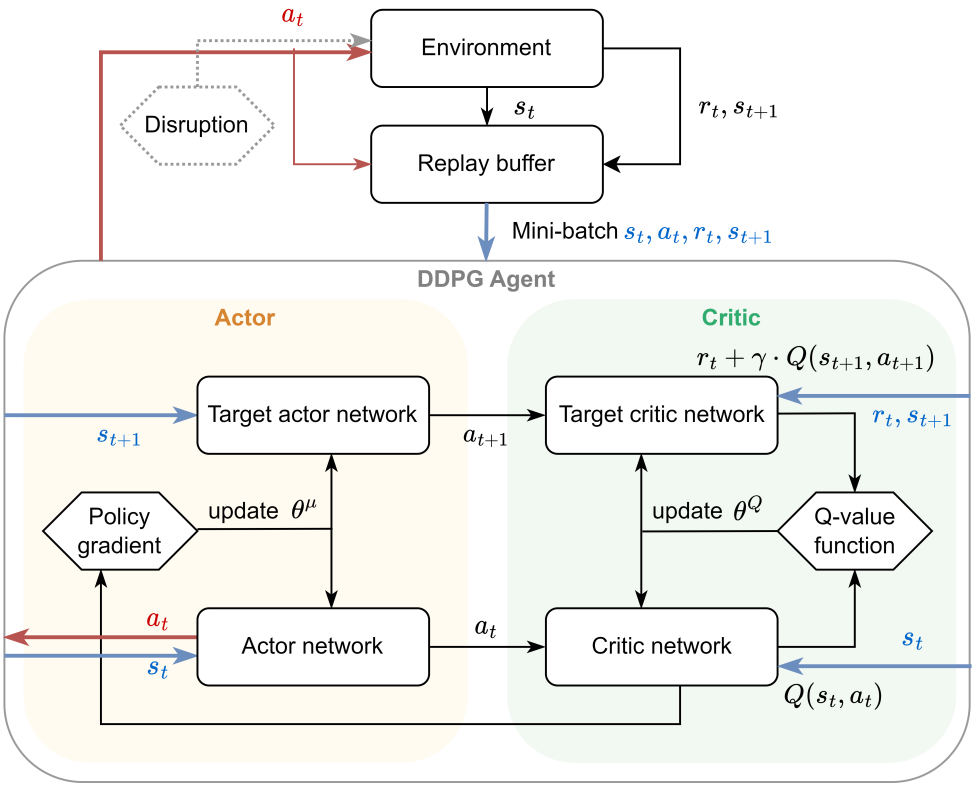

FIGURE 2: DDPG scheme

The actor network is represented by $\mu(\cdot)$ and it determines the best action a_t, which is the percentage of vehicles that are allowed to travel across the periphery, based on the current state s_t given the weight θ^μ at a certain time step t:

$$a_t = \mu(s_t|\theta^\mu) \tag{11}$$

The critic network, denoted by $Q(\cdot)$, takes the responsibility to evaluate whether a specific state-action pair at a certain time step yields the maximal possible discounted future reward $Q(s_t, a_t)$. A common technique used in DDPG is to create a target actor network $\mu'(\cdot)$ and a target critic network $Q'(\cdot)$, which are a copy of the original actor and critic network but updated posteriorly to stabilize the training process and prevent overfitting (*91*). The target maximal discounted future reward for the target critic network can be calculated as in Eq. 12.

$$y_i = r_i + \gamma Q'(s_{i+1}, \mu'(s_{i+1}|\theta^{\mu'})|\theta^{Q'}) \tag{12}$$

Similar to DQN, the critic network can be updated through calculating the temporal difference between the predicted reward and the target reward and minimizing the loss for a mini-batch N sampled from the replay buffer:

$$L = \frac{1}{N}\sum_i (y_i - Q(s_i, a_i|\theta^Q))^2 \tag{13}$$

Afterward, the actor network can be updated with sampled deterministic policy gradient (*92*):

$$I = \mathbb{E}_{s_t \sim \rho^\beta}[r(s, \mu(s|\theta^\mu))|_{s=s_t}] \tag{14}$$

$$\nabla_{\theta^\mu} I = \mathbb{E}_{s_t \sim \rho^\beta}[\nabla_a Q(s,a|\theta^Q)|_{s=s_t, a=\mu(s_t)} \nabla_{\theta_\mu} \mu(s|\theta^\mu)|_{s=s_t}] \tag{15}$$

$$\nabla_{\theta^\mu} I \approx \frac{1}{N} \sum_t \nabla_a Q(s,a|\theta^Q)|_{s=s_t, a=\mu(s_t)} \nabla_{\theta^\mu} \mu(s|\theta^\mu)|_{s_t} \tag{16}$$

When training the agent, we add intermittent disruptions into the simulation environment at certain training episodes, in the form of a temporary surging traffic demand. The following Algorithm 1 summarizes all the essential steps to implement the DDPG algorithm under the scenario with the assumption of disruption occurrences.

Antifragility and the antifragile terms in RL

In this paper, we demonstrate the two types of antifragility as introduced in Section 3. We refer to the antifragility gained from experiencing disruptions sequentially as antifragility type I, and the nonlinear response of linearly increasing disruptions regardless of prior experience as antifragility type II.

As illustrated in Section 3, researchers have been working around the state space $\mathscr{S}$ of the RL algorithms to induce robustness of various traffic control strategies (*60, 62–64*). In our work, following the same logic, we add additional terms based on derivatives (*8*) and redundancy (*76*), in the state space $\mathscr{S}$ and the reward function $\mathscr{R}$ of the RL algorithm.

For the state space $\mathscr{S}$, the baseline RL algorithm (*51*) uses traffic demand q_{ij} as additional information fed to the agent other than accumulation n_{ij}. In our work, we replace q_{ij} using the first and second derivatives of the vehicle accumulation $dn_{ij}(t)$ and $d^2n_{ij}(t)$. With this additional information, the RL agent is aware of a possible demand surge and $d^2n_{ij}(t)$ can reflect the curvature of the demand profile, i.e., how fast the demand is soaring so that the agent would anticipate the possible magnitude of demand in the future time steps.

For the reward function $\mathscr{R}$, the trip completion at each time step acts as the main component as in MPC. The term $\varepsilon(t)$ in the objective function J_{RL} in Equation (10) acts as an additional term to build up redundancy in the system. Similar to the creation of the additional term in the state space, we create redundancy also through the calculation of the derivates, but instead of the derivatives of the vehicle accumulation, we calculate the derivatives of the traffic state. First, we summarize $\varepsilon(t)$ as the sum of two terms, with $H(t)$ being an overall term representing the first derivative of the traffic state and $\Delta H(t)$ representing the second derivative:

$$\varepsilon(t) = H(t) + \Delta H(t) \tag{21}$$

$H(t)$ and $\Delta H(t)$ can be expanded as:

$$H(t) = \sum_{i=1,2} H_i(t) = \omega_h \sum_{i=1,2} f(n_i(t), n_{i,crit}, n_{i,cap}) \cdot \alpha_i(t) \cdot h_i(t) \tag{22}$$

$$\Delta H(t) = \sum_{i=1,2} \Delta H_i(t) = \omega_{\Delta h} \sum_{i=1,2} f(n_i(t), n_{i,crit}, n_{i,cap}) \cdot \Delta h_i(t) \tag{23}$$

$h_i(t)$ and $\Delta h_i(t)$ are the first and second numerical derivatives of the traffic states on the MFD, $h_i(t)$ is defined as the difference of trip completion over vehicle accumulation at the end of a time step versus at the beginning of the same time step, as in Eq. 24 shows, and the second

Algorithm 1 RL-based algorithm for perimeter control with disruption occurrence

Initialize actor $\mu(s|\theta^{\mu})$ and critic network $Q(s,a|\theta^{Q})$ with random weight θ^{Q}, θ^{μ}
Initialize target actor network μ' and target critic network Q' with the same weight
Initialize the replay memory, converge_flag
for episode = 1 **to** max_epi **do**
  Initialize a normal distribution N as random noise for action exploration
  Receive initial observation and reward s_1, r_1 through the agent interacting with environment
  for t = 1 **to** max_step **do**
    Choose action $a_t = \mu(s_t|\theta^{\mu})$ with noise n_t
    if disruption = True **then**
      Update the demand profile regarding the predefined disruption

$$q(t) \leftarrow q(t) + q_{dist}(t) \tag{17}$$

    end if
    Agent interacting with the environment and gets reward r_t and new state s_{t+1}
    Record (s_t, a_t, r_t)
    if Training = True **then**
      Store into the replay memory and get a mini-batch (s_i, a_i, r_i, s_{i+1})
      Determining maximal future reward with target actor and critic network

$$y_i = r_i + \gamma Q'(s_{i+1}, \mu'(s_{i+1}|\theta\mu')|\theta^{Q'}) \tag{18}$$

      Update critic network weight θ^{Q} by minimizing the loss

$$L = \frac{1}{N}\sum_i (y_i - Q(s_i, a_i|\theta^{Q}))^2 \tag{19}$$

      Update the actor network weight θ^{μ} through policy gradient

$$\nabla_{\theta^{\mu}} I \approx \frac{1}{N}\sum_t \nabla_a Q(s,a|\theta^{Q})|_{s=s_t, a=\mu(s_t)} \nabla_{\theta^{\mu}} \mu(s|\theta^{\mu})|_{s_t} \tag{20}$$

      Update the target actor network and target critic network
    end if
  end for
  Test the performance on the same environment and check convergence
  if episode = converge_episode and converge_flag = False **then**
    Abort
  end if
end for

derivative $\Delta h_i(t)$ is calculated as the difference between the first derivatives of two consecutive time steps, as in Eq. 25 shows:

$$h_i(t) = \frac{M_i(t) \; - \; M_i(t-1)}{n_i(t) \; - \; n_i(t-1)} \tag{24}$$

$$\Delta h_i(t) = h_i(t) - h_i(t-1) \tag{25}$$

Since in the RL algorithms implemented in this paper, all variables involved in the deep neural network should be normalized to facilitate the training process, meaning the exact values of the derivatives are not of importance, ω_h and $\omega_{\Delta h}$ are introduced as the weight constants for the

first and second derivatives to regulate their impact on the reward side $\mathscr{R}$.

$\alpha_i(t)$ is a binary variable designed in the first derivative to reward the agent when moving towards the desired direction on the MFD. For instance, the derivative of any data point in the congested zone of the MFD is negative. In this case, when the vehicle accumulation is still getting larger, a penalty will be applied. However, if the vehicle accumulation is decreasing through perimeter control, this binary $\alpha_i(t)$ variable will turn it into a reward. For the second derivative, an additional binary variable is not necessary since the two consecutive first derivatives are able to determine whether $\Delta h_i(t)$ is either positive or negative.

$$\alpha_i(t) = \begin{cases} 1, & \text{if } n_i(t) \geq n_i(t-1), \\ -1, & \text{otherwise.} \end{cases} \tag{26}$$

The term $f(n_i(t), n_{i,crit}, n_{i,cap})$ is a reduction factor to constrain the impact of the $\varepsilon(t)$ term when the accumulation is either on a very lower level or on a very higher level (gridlock). The area around critical accumulation is where the $\varepsilon(t)$ term should have the greatest impact. Here we use a modified trigonometric function to realize this purpose. It should be noted that other functions, such as normal distribution, are also valid for achieving the same purpose.

$$f(n_i(t), n_{i,crit}, n_{i,cap}) = \begin{cases} \dfrac{1+\cos(-\pi \cdot \dfrac{n_{i,crit} - n_i(t)}{n_{i,crit}})}{2}, & \text{if } n_i(t) \geq n_{i,crit}, \\ \dfrac{1+\cos(-\pi \cdot \dfrac{n_i(t) - n_{i,crit}}{n_{i,cap} - n_{i,crit}})}{2}, & \text{otherwise.} \end{cases} \tag{27}$$

After considering all the modifiers above, we show $H(t)$ and $\Delta H(t)$ using a single MFD as an example in Figure 3.

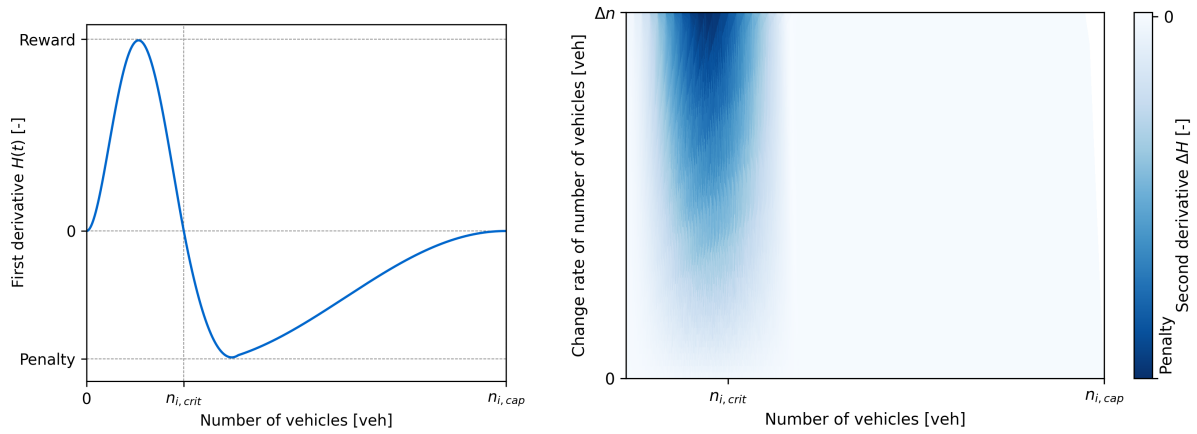

(a) Overall term H for the first derivative $h_i(t)$ (b) Overall term ΔH for the second derivative $\Delta h_i(t)$

FIGURE 3: Illustration of overall term $H(t)$ and $\Delta H(t)$ on the reward $\mathscr{R}$

As can be noticed, the first derivative $H(t)$, in Figure 3a, rewards the agent more when it's moving towards the critical accumulation to maximize its trip completion rate. However, when the number of vehicles approaches the critical accumulation, the reward drops significantly and

becomes a penalty when it exceeds the critical point. For the second derivative $\Delta H(t)$ in Figure 3b, it always applies a penalty to the agent, and a darker blue indicates a greater penalty. The x-axis is the accumulation, same as in Figure 3a, while the y-axis represents how fast the traffic state is changing on the MFD. The faster it changes around the critical accumulation, the greater the penalty will be on the RL agent. With $H(t)$ and $\Delta H(t)$, the agent learns to be conservative when regulating the perimeter control variables when the accumulation is about to reach critical, in case of disruptions take place. Therefore, as can be concluded, although $H(t)$ and $\Delta H(t)$ apply the same concept of the derivative as the $dn_{ij}(t)$ and d^2n_{ij} in the state space $\mathscr{S}$, the purpose of $H(t)$ and $\Delta H(t)$ is preserving redundancy in the system instead of feeding additional information to the agent.

EXPERIMENT APPLICATION

This section introduces the environment setup of the simulation and the evaluation procedure. We investigate a total number of three perimeter control strategies in addition to a no-control scenario, based on 2 different scenarios, i.e., under constant or incremental disruptions for testing antifragility type I and type II respectively. The model-based approach utilized is Model Predictive Control (MPC), whereas the other two perimeter control strategies are based on RL. While both of these RL-based methods adopt the same definition of action $a_t \in \mathscr{A}$ as the perimeter control variable, the definition of state $\mathscr{S}$ and reward $\mathscr{R}$ differ between the methods.

- No control
- MPC modified from Geroliminis et al. (*22*), averaging history demand profile
- State-of-the-art RL-based method proposed by Zhou and Gayah (*51*) as baseline:
  State s_t: vehicle accumulation and traffic demand $[n_{ij}(t), q_{ij}(t)]$
  Reward r_t: trip completion in both regions $[\sum_{i=1,2} M_{ii}(t)]$
- Our proposed RL-based antifragile method:
  State s_t: vehicle accumulation and the first and second derivatives $[n_{ij}(t), dn_{ij}(t), d^2n_{ij}(t)]$
  Reward r_t: trip completion and the $\varepsilon(t)$ term $[\sum_{i=1,2} M_{ii}(t) + \varepsilon(t)]$

Simulation environment

We simulate a cordon-shaped urban network with inner and outer regions with different MFDs, which resemble those in (*51*). Some minor modifications have been adapted in the congested zone of the MFD to ensure the derivative of the MFD is continuous. The MFD of the outer region is largely in line with the observations in Yokohama (*20*). Other critical indicators, e.g., critical accumulation and maximal trip completion, remain unchanged. The non-identical MFDs reflect the fact that the area of the periphery is much larger than the city center, and thus the maximal accumulation would be significantly higher. The traffic demand under no disruption is modified based on (*20*). Instead of a trapezoidal demand profile, the chosen profile is in the shape of a normal distribution in accordance with (*93*) to describe the peak hour traffic flow. The total simulation duration t_{end} is 2 hours with each time step Δt as 60 seconds, and the second hour has significantly fewer vehicles so that the network would be able to clear the vehicles accumulated in the first hour. Other notable constraints and initializations include the lower and upper bounds for the perimeter control variable $u_{ij} \in [0.1, 0.9]$ (*22*) and an initial accumulation in the network $n_{ij,0} = [600, 1300, 300, 2400]$.

Two different scenarios are considered in this work. For the validation of antifragility type I, after the agent has been trained for the first 50 episodes with a base demand profile, as

shown in Figure 4a, we introduce a new demand profile with disruption, which characterizes a surging demand within a short period of time from the outer region into the inner region. The new environment lasts for 50 episodes with the disruption being a constant magnitude of 2500 vehicles following normal distribution, as shown in Figure 4b. To test antifragility type II, with the total number of episodes being the same 100 episodes, instead of a constant amplitude of disruption, an incremental disruption is applied for the last 50 episodes. The amplitude of disruption grows linearly from 0 to twice the number of vehicles in the scenario with constant disruptions. Both the RL-based methods are trained 15 times and the average is calculated as their learning curves.

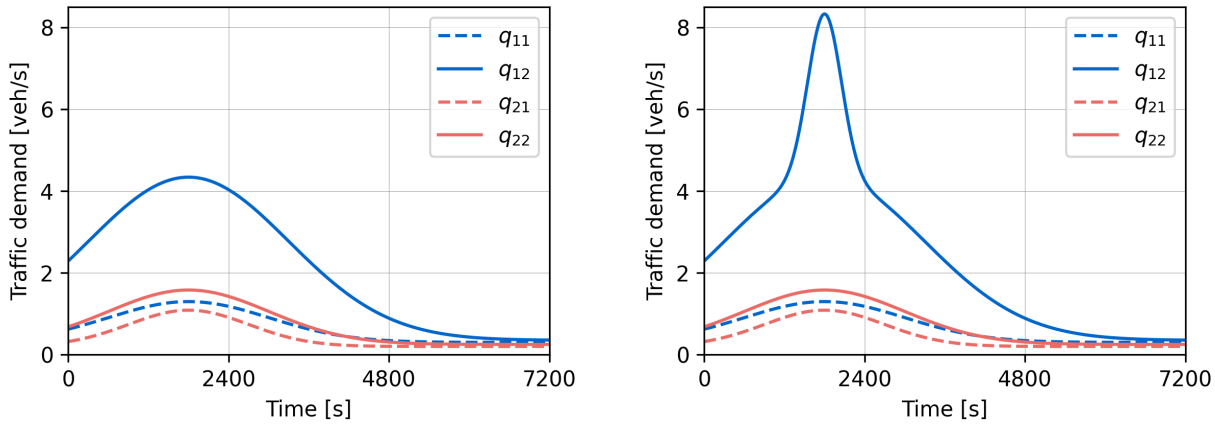

(a) Base demand profile

(b) Demand profile under demand disruption

FIGURE 4: Demand profile with or without disruption

Performance evaluation

Although the reward defined in the RL algorithm is based on trip completion, to better showcase antifragility, the main performance indicator being evaluated here is the total time spent (TTS), which is calculated by adding the number of vehicles within the network at each second of the simulation. The main reason for choosing TTS over completion is that completion is lower bounded with increasing magnitude of disruption by the number of vehicles that finished their trips before the disruption, which means we may observe a concave trip completion with increasing disruptions at first but then it becomes approximately constant. This makes the manifestation of antifragility difficult since the performance curve could be partially concave and partially convex. However, by using TTS as the performance indicator, we circumvent this problem since TTS still grows linearly with increasing disruptions even under extreme cases instead of being lower-bounded. Therefore, the full convexity or concavity of the performance curve can be maintained and we can roughly approximate the simulation results with a second-degree polynomial.

As urban road networks are always subject to capacity constraints, fully antifragile traffic control strategies may be impossible to design. Therefore, we normalize all the other perimeter control strategies over the RL baseline method to study the relative antifragility. To quantify the antifragility type II of different methods, we calculate the skewness of the TTS distribution. A more negative value of skewness indicates the distribution has a longer or fatter left tail and thus a higher degree of concavity in the function.

RESULTS

This section presents the simulation results of the four methods, i.e., no-control, MPC, baseline RL-based method, and our proposed antifragile RL-based method under the two scenarios to show the property of antifragility type I and antifragility type II, respectively.

Antifragility type I

Systems with the property of antifragility type I can learn from past adverse events and anticipate possible ongoing disruptions to enhance future performance. To test this property, we apply disruptions with constant magnitude after training with the base demand profile.

Unlike the no-control and MPC approaches, RL-based methods are subject to performance variations over simulation episodes. Therefore, in Figure 5, other than the performance curves of the no-control and MPC approaches, we show the learning curves of the baseline RL method and our proposed antifragile RL method. The curves are averaged from 15 simulations, while the shadowed area indicates the standard deviation of the simulation results. After conducting 50 episodes of training together with testing, an additional 2 testing phases were implemented using the final weight parameters obtained from the training process. These tests were performed under or under no disruptions.

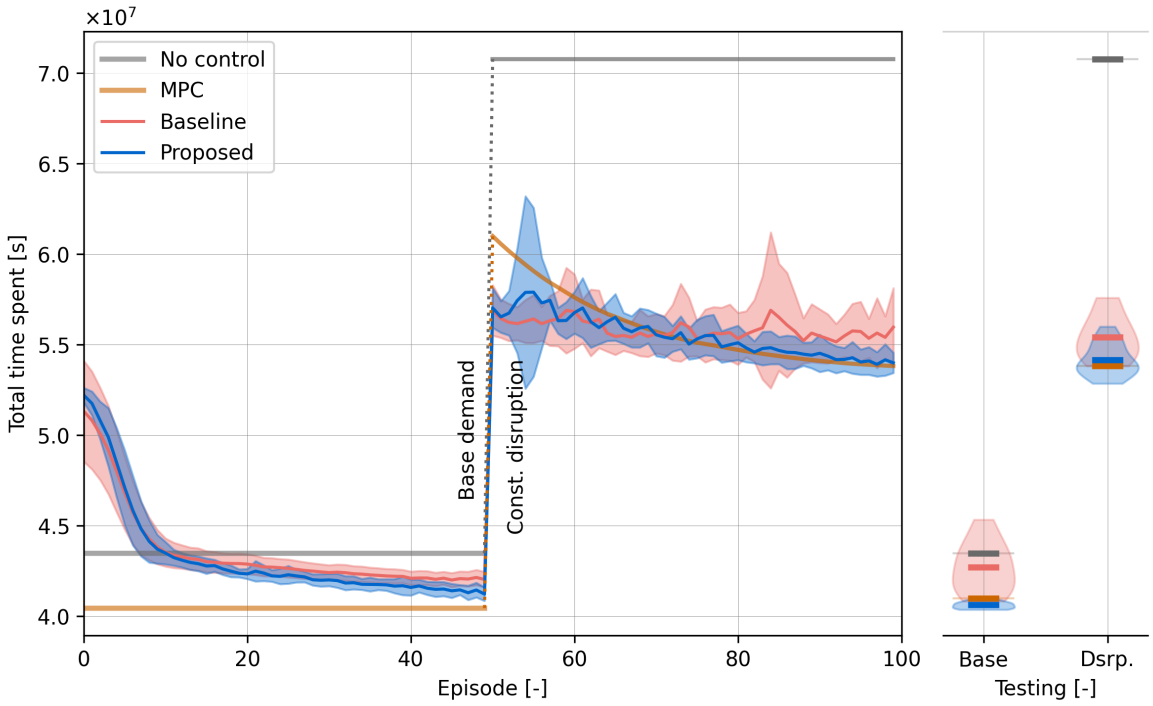

FIGURE 5: Learning curves under constant disruptions

It can be noticed that two significant phenomena occur during the initial 50 episodes with the base demand profile. First, the proposed antifragile method can achieve better performance with less TTS when there is no disruption in the network. While the baseline method has almost converged after 50 episodes, the proposed antifragile method seems to be capable of further improving the performance with more training episodes. The reason for not continuing the training

process until the convergence of both methods is to avoid overtraining the non-disruption-related weight parameters as well as the underfitting of the disruption-related parameters. Regardless of the better performance of the proposed method, the shadowed area represents a more significant performance variation compared to the baseline method, indicating that our proposed antifragile method exhibits comparably lower training stability.

After disruption with constant magnitude is introduced into the network. The performance of the two RL-based methods has first changed drastically. Then, while the proposed method has an obvious tendency of reducing TTS over 50 episodes, the baseline method shows no clear sign of improving performance. In contrast to the conclusion above, the proposed method has a higher training stability compared to the baseline method and also becomes increasingly stable over episodes as the width of the shadowed area is getting smaller.

While the results of testing under disruption follow the same pattern as the last episode of the training process, however, when the simulation environment reverts to the previous no-disruption condition, the performance of different methods behaves differently. Since our modified MPC averages demand history, after experiencing episodes with disruptions, the performance deteriorates when there is no disruption. A similar pattern can be observed for the baseline RL method. Not only is the TTS higher in this testing episode compared to the training episode 50, but the performance variation is also significantly larger. On the contrary, our proposed antifragile RL method can both maintain excellent performance and achieve smaller variation.

We normalize all the other methods over the result of the baseline RL-based method averaged from the 15 simulations, as shown in Figure 6. The performance improvement of both MPC and the proposed antifragile methods can be observed. Since we average all the past experiences of the demand profile, including disruptions for MPC, it is capable of performing better under the same disrupted scenario, and even marginally better than the proposed antifragile method, demonstrating the property of antifragility type I. While maintaining roughly similar performance compared to the baseline method at the beginning of the scenario switch, and thus better performance than MPC, the proposed method gains capability in dealing with disruptions when experiencing more and more such disruptions, also showing the property of being antifragile.

Antifragility type II

Antifragility type II describes a system that exhibits a nonlinear response to a linearly increasing magnitude of disruptions. In terms of TTS, since an increase in the traffic density or vehicle accumulation in the network will inevitably lead to a decrease in the vehicle speed or trip completion rate based on the speed MFD, therefore, a concave response between TTS and vehicle accumulation indicates an antifragile type II system. The four studied methods are tested in an environment with linearly increasing traffic demand for 50 episodes after being trained with the same base demand as in the previous scenario for 50 episodes. furthermore, another testing phase of 20 episodes is carried out following the same demand increment and the demand magnitude of the last training episode. Figure 7a shows the TTS of different methods under incremental disruptions in both training and testing phases. It should be noted that Figure 7a and Figure **??** do not share the same y-axis and the result of the no-control approach is not presented in **??** due to its exceedingly high value.

Under this scenario, the TTS of the no-control approach grows sharply, doubling the difference between the last and the first episode under the incremental disruption of the other methods. Similar to the previous scenario, the performance deviation of the proposed method is relatively

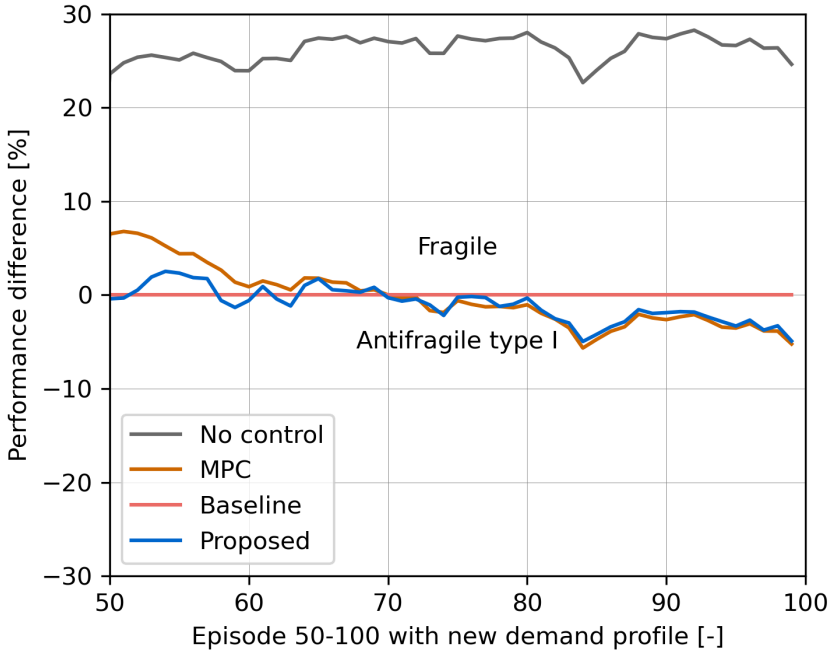

FIGURE 6: Performance difference normalized over the baseline method under constant disruptions

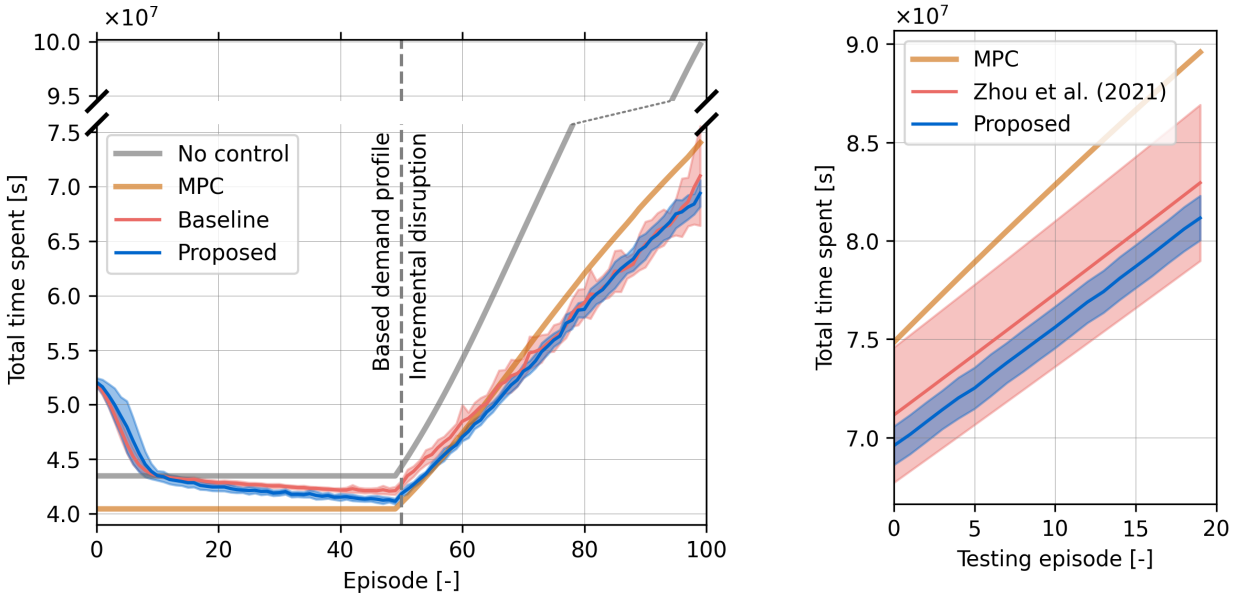

(a) Training for 50 episodes

(b) Testing for additional 20 episodes

FIGURE 7: Learning curves under incremental disruptions

lower compared to the baseline method under the disruptions scenario. However, one more phenomenon to notice is that under incremental disruptions, the performance deviation of both meth-

ods also grows with the increase in the magnitude of disruption. And the deviation of the baseline method is significantly higher compared to the proposed antifragile method in the last simulation episodes. Although the performance of MPC under the constant disruptions scenario is even marginally better than the proposed antifragile method, the performance falls behind the other 2 RL-based methods, as the amplitude of the disruption remains low and grows linearly after the first 50 episodes. Therefore, When averaging the past disruption experiences, MPC cannot gain sufficient knowledge of the upcoming magnitude of the disruptions. In the testing phase, it can be observed that the performance deviation of the baseline RL method is significantly larger compared to the proposed antifragile RL method. But since the weight parameters of the agents in the testing phase are not updated anymore, this could be a reason that the performance curves of the RL-based methods appear to be linear.

Since the performance differences between the baseline and the other methods are hard to observe in this figure, we need to normalize the performance of all the other methods over the baseline methods. Before the normalization process, to better showcase the nonlinear response and compare the concavity or convexity of different methods, the performance deviation in the learning curves of the RL-based methods needs to be minimized. Therefore, we approximate the simulation results of different methods each with a second-degree polynomial, and recreate the data points after fitting the polynomial coefficients, with which the normalization process can be implemented, and the results are shown in Figure 8.

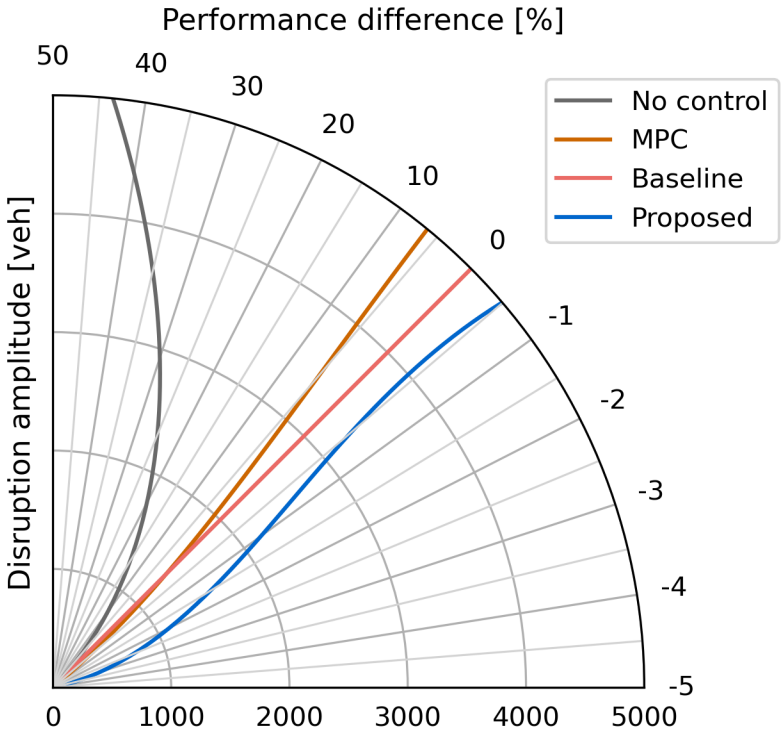

FIGURE 8: Performance difference normalized over the baseline method under incremental disruptions

One of the benefits of a polar coordinate system over the cartesian coordinates is that it amplifies the performance difference, particularly when the disruption magnitude is high, and this

region is where we pay the most attention. While both the no-control approach and MPC have a positive increasing performance difference in comparison to the baseline method. The proposed antifragile method is the only one that remains a negative difference with its absolute value growing even larger after the disruption reaches around 4000 vehicles. However, it should be first noted that due to the characteristics of the polar coordinates, a concave or convex curve on this plot does not necessarily indicates that the data points of a specific method follow a concave or convex distribution. A linearly increasing curve can demonstrate itself as a spiral curve in the polar coordinates. Nevertheless, it can also be observed that the curve of the proposed method first draws near to the baseline curve and has, for instance, a performance difference of -0.5% under the disruption with roughly 3200 additional vehicles, then it recedes at some point, and reaches -0.5% again with around 5000 vehicles. This indicates that the proposed method has a relative concavity compared to the baseline method, showcasing the antifragility type II.

To quantify the antifragility type II of our proposed method, we demonstrate the distribution of performance difference in Figure 9. The proposed antifragile method exhibits the most concentrated distribution, indicating a lower TTS on average compared to the other methods under the same disruptions.

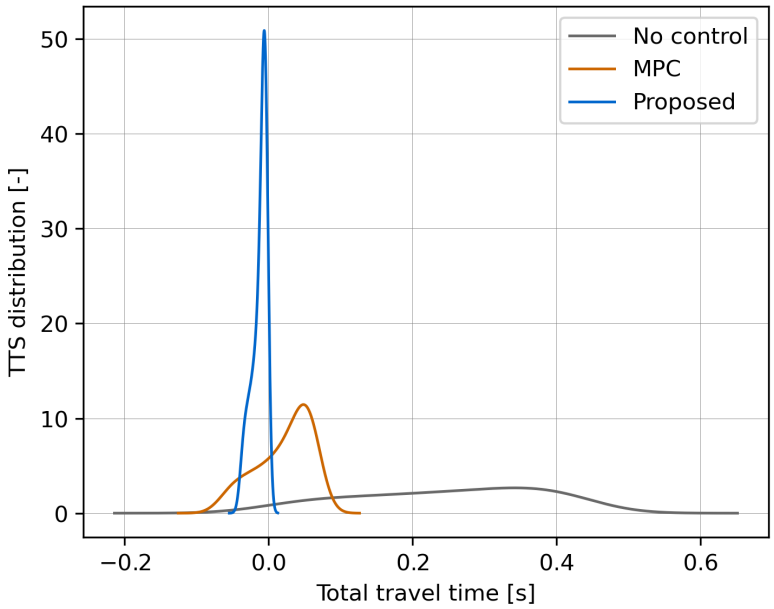

FIGURE 9: Distribution of TTS

Moreover, in order to compare the (anti)fragility among different methods quantitively, we calculate the skewness of each distribution. In Table 4, we summarize the skewness of each studied method. Surprisingly, all 3 methods possess a negative skewness, indicating a relative antifragility type II compared to the baseline method. In other words, the baseline method is the most fragile of all the 4 methods investigated in this study. While the no-control approach has the least relative antifragility, our proposed antifragile method has demonstrated the strongest antifragility property, with its skewness of distribution being the most negative of all.

TABLE 4: Normalized Skewness over Baseline Method under Incremental Disruptions

Methods	Skewness
No control	-0.326
MPC	-0.753
Antifragile RL-based method	-1.106

CONCLUSION

First, this research work introduces the concept of antifragility by comparing it with two other terms robustness and resilience, which are commonly used in transportation and traffic control strategies. Through a literature review on using RL algorithms in traffic control to realize a robust or resilient design, whether and how such properties can be induced in RL is investigated. Following the same idea, we manage to induce antifragility in perimeter control by modifying the state space and reward function based on a state-of-the-art RL-based perimeter control strategy. We incorporate the change rate and curvature of the traffic states in the state space to leverage the potential of such derivatives to feed more information to the RL algorithm. Also, a redundancy term in the reward function has been carefully composed to empower the system to be more resistant to disruptions.

We conducted a comprehensive comparison between our proposed antifragile RL-based perimeter control approach and three other methods: no-control, MPC, and a baseline RL-based method. This comparison was carried out under two different scenarios, disruptions with constant and incremental magnitude, for validating the antifragility type I and type II individually. The results from the study clearly demonstrated the effectiveness and antifragility of our proposed method, for both antifragility type I and type II. Furthermore, we put forward a novel method for quantifying antifragility, utilizing the measure of skewness in the distribution. Our proposed antifragile method exhibits the greatest negative skewness among the methods examined, indicating its relative antifragility property against disruptions.

In conclusion, this study is the first of its kind to pioneer the application of the antifragility concept in enhancing the daily operation of engineering systems to enhance performance during unforeseen disruptions using a learning-based algorithm. It introduces a new possibility for evaluating system operation under disruptive conditions. Moreover, the concept can be extended not only to other traffic control strategies like traffic signal control and pricing but also to various engineering disciplines and industries, broadening its potential impact.

REFERENCES

1. Figueiredo, L., I. Jesus, J. Machado, J. Ferreira, and J. Martins de Carvalho, Towards the development of intelligent transportation systems. In *ITSC 2001. 2001 IEEE Intelligent Transportation Systems. Proceedings (Cat. No.01TH8585)*, 2001, pp. 1206–1211.
2. Haque, M. M., H. C. Chin, and A. K. Debnath, Sustainable, safe, smart—three key elements of Singapore's evolving transport policies. *Transport Policy*, Vol. 27, 2013, pp. 20–31.
3. Qureshi, K. and H. Abdullah, A Survey on Intelligent Transportation Systems. *Middle-East Journal of Scientific Research*, Vol. 15, 2013, pp. 629–642.
4. Ganin, A. A., A. C. Mersky, A. S. Jin, M. Kitsak, J. M. Keisler, and I. Linkov, Resilience in Intelligent Transportation Systems (ITS). *Transportation Research Part C: Emerging Technologies*, Vol. 100, 2019, pp. 318–329.
5. Federal Statistical Office, *Mobilität und Verkehr: Panorama (in German/French only)*. 16704292, Neuchâtel, 2020.
6. Chang, G.-L. and H. Xiang, *The relationship between congestion levels and accidents*, 2003.
7. Taleb, N. N., 'Antifragility' as a mathematical idea. *Nature*, Vol. 494, No. 7438, 2013, pp. 430–430, number: 7438 Publisher: Nature Publishing Group.
8. Taleb, N. N. and R. Douady, Mathematical definition, mapping, and detection of (anti)fragility. *Quantitative Finance*, Vol. 13, No. 11, 2013, pp. 1677–1689, publisher: Routledge _eprint: https://doi.org/10.1080/14697688.2013.800219.
9. Aven, T., The Concept of Antifragility and its Implications for the Practice of Risk Analysis. *Risk Analysis*, Vol. 35, No. 3, 2015, pp. 476–483, _eprint: https://onlinelibrary.wiley.com/doi/pdf/10.1111/risa.12279.
10. Zhu, L., F. R. Yu, Y. Wang, B. Ning, and T. Tang, Big Data Analytics in Intelligent Transportation Systems: A Survey. *IEEE Transactions on Intelligent Transportation Systems*, Vol. 20, No. 1, 2019, pp. 383–398, conference Name: IEEE Transactions on Intelligent Transportation Systems.
11. Yuan, T., W. Da Rocha Neto, C. E. Rothenberg, K. Obraczka, C. Barakat, and T. Turletti, Machine learning for next-generation intelligent transportation systems: A survey. *Transactions on Emerging Telecommunications Technologies*, Vol. 33, No. 4, 2022, p. e4427, _eprint: https://onlinelibrary.wiley.com/doi/pdf/10.1002/ett.4427.
12. Haydari, A. and Y. Yılmaz, Deep Reinforcement Learning for Intelligent Transportation Systems: A Survey. *IEEE Transactions on Intelligent Transportation Systems*, Vol. 23, No. 1, 2022, pp. 11–32, conference Name: IEEE Transactions on Intelligent Transportation Systems.
13. Sutton, R. S. and A. G. Barto, *Reinforcement Learning, second edition: An Introduction*. MIT Press, 2018, google-Books-ID: uWV0DwAAQBAJ.
14. Li, Y., *Deep Reinforcement Learning: An Overview*, 2018, arXiv:1701.07274.
15. Mysore, S., B. Mabsout, R. Mancuso, and K. Saenko, Regularizing Action Policies for Smooth Control with Reinforcement Learning. In *2021 IEEE International Conference on Robotics and Automation (ICRA)*, 2021, pp. 1810–1816, iSSN: 2577-087X.
16. O'dwyer, A., *Handbook Of Pi And Pid Controller Tuning Rules (3rd Edition)*. World Scientific, 2009.

17. Bemporad, A., Model Predictive Control Design: New Trends and Tools. In *Proceedings of the 45th IEEE Conference on Decision and Control*, 2006, pp. 6678–6683, iSSN: 0191-2216.
18. Wang, H., C. R. Wang, M. Zhu, and W. Hong, Globalized Modeling and Signal Timing Control for Large-scale Networked Intersections. In *Proceedings of the 2nd ACM/EIGSCC Symposium on Smart Cities and Communities*, ACM, Portland OR USA, 2019, pp. 1–7.
19. Daganzo, C. F., Urban gridlock: Macroscopic modeling and mitigation approaches. *Transportation Research Part B: Methodological*, Vol. 41, No. 1, 2007, pp. 49–62.
20. Geroliminis, N. and C. F. Daganzo, Existence of urban-scale macroscopic fundamental diagrams: Some experimental findings. *Transportation Research Part B: Methodological*, Vol. 42, No. 9, 2008, pp. 759–770.
21. Knoop, V. L., S. P. Hoogendoorn, and J. W. C. Van Lint, Routing Strategies Based on Macroscopic Fundamental Diagram. *Transportation Research Record*, Vol. 2315, No. 1, 2012, pp. 1–10, publisher: SAGE Publications Inc.
22. Geroliminis, N., J. Haddad, and M. Ramezani, Optimal Perimeter Control for Two Urban Regions With Macroscopic Fundamental Diagrams: A Model Predictive Approach. *IEEE Transactions on Intelligent Transportation Systems*, Vol. 14, No. 1, 2013, pp. 348–359, conference Name: IEEE Transactions on Intelligent Transportation Systems.
23. Kouvelas, A., M. Saeedmanesh, and N. Geroliminis, Enhancing model-based feedback perimeter control with data-driven online adaptive optimization. *Transportation Research Part B: Methodological*, Vol. 96, 2017, pp. 26–45.
24. Yang, K., N. Zheng, and M. Menendez, Multi-scale Perimeter Control Approach in a Connected-Vehicle Environment. *Transportation Research Procedia*, Vol. 23, 2017, pp. 101–120.
25. Zheng, N., R. A. Waraich, K. W. Axhausen, and N. Geroliminis, A dynamic cordon pricing scheme combining the Macroscopic Fundamental Diagram and an agent-based traffic model. *Transportation Research Part A: Policy and Practice*, Vol. 46, No. 8, 2012, pp. 1291–1303.
26. Zheng, N. and N. Geroliminis, Modeling and optimization of multimodal urban networks with limited parking and dynamic pricing. *Transportation Research Part B: Methodological*, Vol. 83, 2016, pp. 36–58.
27. Genser, A. and A. Kouvelas, Dynamic optimal congestion pricing in multi-region urban networks by application of a Multi-Layer-Neural network. *Transportation Research Part C: Emerging Technologies*, Vol. 134, 2022, p. 103485.
28. Yildirimoglu, M., M. Ramezani, and N. Geroliminis, Equilibrium Analysis and Route Guidance in Large-scale Networks with MFD Dynamics. *Transportation Research Procedia*, Vol. 9, 2015, pp. 185–204.
29. Fu, H., S. Chen, K. Chen, A. Kouvelas, and N. Geroliminis, Perimeter Control and Route Guidance of Multi-Region MFD Systems With Boundary Queues Using Colored Petri Nets. *IEEE Transactions on Intelligent Transportation Systems*, Vol. 23, No. 8, 2022, pp. 12977–12999, conference Name: IEEE Transactions on Intelligent Transportation Systems.
30. Hajiahmadi, M., V. L. Knoop, B. De Schutter, and H. Hellendoorn, Optimal dynamic route guidance: A model predictive approach using the macroscopic fundamental diagram. In

16th International IEEE Conference on Intelligent Transportation Systems (ITSC 2013), 2013, pp. 1022–1028, iSSN: 2153-0017.

31. Ambühl, L., A. Loder, M. Menendez, and K. W. Axhausen, A case study of Zurich's two-layered perimeter control, 2018, p. 8 p., artwork Size: 8 p. Medium: application/pdf Publisher: ETH Zurich.
32. Keyvan-Ekbatani, M., A. Kouvelas, I. Papamichail, and M. Papageorgiou, Exploiting the fundamental diagram of urban networks for feedback-based gating. *Transportation Research Part B: Methodological*, Vol. 46, No. 10, 2012, pp. 1393–1403.
33. Sirmatel, I. I. and N. Geroliminis, Nonlinear Moving Horizon Estimation for Large-Scale Urban Road Networks. *IEEE Transactions on Intelligent Transportation Systems*, Vol. 21, No. 12, 2020, pp. 4983–4994, conference Name: IEEE Transactions on Intelligent Transportation Systems.
34. Ambühl, L., A. Loder, N. Zheng, K. W. Axhausen, and M. Menendez, Approximative Network Partitioning for MFDs from Stationary Sensor Data. *Transportation Research Record*, Vol. 2673, No. 6, 2019, pp. 94–103, publisher: SAGE Publications Inc.
35. Saedi, R., M. Saeedmanesh, A. Zockaie, M. Saberi, N. Geroliminis, and H. S. Mahmassani, Estimating network travel time reliability with network partitioning. *Transportation Research Part C: Emerging Technologies*, Vol. 112, 2020, pp. 46–61.
36. Aboudolas, K. and N. Geroliminis, Feedback perimeter control for multi-region large-scale congested networks. In *2013 European Control Conference (ECC)*, 2013, pp. 3506–3511.
37. Haddad, J. and B. Mirkin, Coordinated distributed adaptive perimeter control for large-scale urban road networks. *Transportation Research Part C: Emerging Technologies*, Vol. 77, 2017, pp. 495–515.
38. Ambühl, L., A. Loder, L. Leclercq, and M. Menendez, Disentangling the city traffic rhythms: A longitudinal analysis of MFD patterns over a year. *Transportation Research Part C: Emerging Technologies*, Vol. 126, 2021, p. 103065.
39. Wang, P., K. Wada, T. Alamatsu, and Y. Hara, An Empirical Analysis of Macroscopic Fundamental Diagrams for Sendai Road Networks. *Interdisciplinary Information Sciences*, Vol. 21, 2015, pp. 49–61.
40. Ji, Y., R. Jiang, E. Chung, and X. Zhang, The impact of incidents on macroscopic fundamental diagrams. *Proceedings of the Institution of Civil Engineers: Transport*, Vol. 168, 2015, pp. 396–405.
41. Gayah, V. V. and C. F. Daganzo, Clockwise hysteresis loops in the Macroscopic Fundamental Diagram: An effect of network instability. *Transportation Research Part B: Methodological*, Vol. 45, No. 4, 2011, pp. 643–655.
42. Baldi, S., I. Michailidis, V. Ntampasi, E. Kosmatopoulos, I. Papamichail, and M. Papageorgiou, A Simulation-Based Traffic Signal Control for Congested Urban Traffic Networks. *Transportation Science*, Vol. 53, No. 1, 2019, pp. 6–20, publisher: INFORMS.
43. Nguyen, H., L.-M. Kieu, T. Wen, and C. Cai, Deep learning methods in transportation domain: a review. *IET Intelligent Transport Systems*, Vol. 12, No. 9, 2018, pp. 998–1004, _eprint: https://onlinelibrary.wiley.com/doi/pdf/10.1049/iet-its.2018.0064.
44. Wei, H., N. Xu, H. Zhang, G. Zheng, X. Zang, C. Chen, W. Zhang, Y. Zhu, K. Xu, and Z. Li, CoLight: Learning Network-level Cooperation for Traffic Signal Control. In *Proceedings of the 28th ACM International Conference on Information and Knowledge Management*, ACM, Beijing China, 2019, pp. 1913–1922.

45. Chen, C., H. Wei, N. Xu, G. Zheng, M. Yang, Y. Xiong, K. Xu, and Z. Li, Toward A Thousand Lights: Decentralized Deep Reinforcement Learning for Large-Scale Traffic Signal Control. *Proceedings of the AAAI Conference on Artificial Intelligence*, Vol. 34, No. 04, 2020, pp. 3414–3421.
46. Wang, Y., H. Jin, and G. Zheng, CTRL: Cooperative Traffic Tolling via Reinforcement Learning. In *Proceedings of the 31st ACM International Conference on Information & Knowledge Management*, Association for Computing Machinery, New York, NY, USA, 2022, CIKM '22, pp. 3545–3554.
47. Zhu, F. and S. V. Ukkusuri, A reinforcement learning approach for distance-based dynamic tolling in the stochastic network environment. *Journal of Advanced Transportation*, Vol. 49, No. 2, 2015, pp. 247–266, _eprint: https://onlinelibrary.wiley.com/doi/pdf/10.1002/atr.1276.
48. Ning, L., Y. Li, M. Zhou, H. Song, and H. Dong, A Deep Reinforcement Learning Approach to High-speed Train Timetable Rescheduling under Disturbances. In *2019 IEEE Intelligent Transportation Systems Conference (ITSC)*, 2019, pp. 3469–3474.
49. Zhu, Y., P. Wang, and F. Corman, A deep reinforcement learning framework for delay management with passenger re-routing, 2021, accepted: 2021-11-24T07:50:01Z.
50. Ni, W. and M. J. Cassidy, Cordon control with spatially-varying metering rates: A Reinforcement Learning approach. *Transportation Research Part C: Emerging Technologies*, Vol. 98, 2019, pp. 358–369.
51. Zhou, D. and V. V. Gayah, Model-free perimeter metering control for two-region urban networks using deep reinforcement learning. *Transportation Research Part C: Emerging Technologies*, Vol. 124, 2021, p. 102949.
52. Clement, A., L. Wioland, V. Govaere, D. Gourc, J. Cegarra, F. Marmier, and D. Kamissoko, Robustness, resilience: typology of definitions through a multidisciplinary structured analysis of the literature. *European Journal of Industrial Engineering*, Vol. 15, No. 4, 2021, pp. 487–513, publisher: Inderscience Publishers.
53. Tang, J., H. Heinimann, K. Han, H. Luo, and B. Zhong, Evaluating resilience in urban transportation systems for sustainability: A systems-based Bayesian network model. *Transportation Research Part C: Emerging Technologies*, Vol. 121, 2020, p. 102840.
54. Testa, A. C., M. N. Furtado, and A. Alipour, Resilience of Coastal Transportation Networks Faced with Extreme Climatic Events. *Transportation Research Record*, Vol. 2532, No. 1, 2015, pp. 29–36, publisher: SAGE Publications Inc.
55. Haghighat, A. K., V. Ravichandra-Mouli, P. Chakraborty, Y. Esfandiari, S. Arabi, and A. Sharma, Applications of Deep Learning in Intelligent Transportation Systems. *Journal of Big Data Analytics in Transportation*, Vol. 2, No. 2, 2020, pp. 115–145.
56. Zhou, Y., J. Wang, and H. Yang, Resilience of Transportation Systems: Concepts and Comprehensive Review. *IEEE Transactions on Intelligent Transportation Systems*, Vol. 20, No. 12, 2019, pp. 4262–4276, conference Name: IEEE Transactions on Intelligent Transportation Systems.
57. Tamvakis, P. and Y. Xenidis, Resilience in Transportation Systems. *Procedia - Social and Behavioral Sciences*, Vol. 48, 2012, pp. 3441–3450.
58. Chen, C., Y. P. Huang, W. H. K. Lam, T. L. Pan, S. C. Hsu, A. Sumalee, and R. X. Zhong, Data efficient reinforcement learning and adaptive optimal perimeter control of network

traffic dynamics. *Transportation Research Part C: Emerging Technologies*, Vol. 142, 2022, p. 103759.

59. Su, Z. C., A. H. F. Chow, C. L. Fang, E. M. Liang, and R. X. Zhong, Hierarchical control for stochastic network traffic with reinforcement learning. *Transportation Research Part B: Methodological*, Vol. 167, 2023, pp. 196–216.
60. Zhou, D. and V. V. Gayah, Scalable multi-region perimeter metering control for urban networks: A multi-agent deep reinforcement learning approach. *Transportation Research Part C: Emerging Technologies*, Vol. 148, 2023, p. 104033.
61. Aslani, M., S. Seipel, M. S. Mesgari, and M. Wiering, Traffic signal optimization through discrete and continuous reinforcement learning with robustness analysis in downtown Tehran. *Advanced Engineering Informatics*, Vol. 38, 2018, pp. 639–655.
62. Chu, T., J. Wang, L. Codecà, and Z. Li, Multi-Agent Deep Reinforcement Learning for Large-Scale Traffic Signal Control. *IEEE Transactions on Intelligent Transportation Systems*, Vol. 21, No. 3, 2020, pp. 1086–1095, conference Name: IEEE Transactions on Intelligent Transportation Systems.
63. Rodrigues, F. and C. L. Azevedo, Towards Robust Deep Reinforcement Learning for Traffic Signal Control: Demand Surges, Incidents and Sensor Failures. In *2019 IEEE Intelligent Transportation Systems Conference (ITSC)*, 2019, pp. 3559–3566.
64. Tan, K. L., A. Sharma, and S. Sarkar, Robust Deep Reinforcement Learning for Traffic Signal Control. *Journal of Big Data Analytics in Transportation*, Vol. 2, No. 3, 2020, pp. 263–274.
65. Wu, C., Z. Ma, and I. Kim, Multi-Agent Reinforcement Learning for Traffic Signal Control: Algorithms and Robustness Analysis. In *2020 IEEE 23rd International Conference on Intelligent Transportation Systems (ITSC)*, 2020, pp. 1–7.
66. Korecki, M., D. Dailisan, and D. Helbing, How Well Do Reinforcement Learning Approaches Cope With Disruptions? The Case of Traffic Signal Control. *IEEE Access*, Vol. 11, 2023, pp. 36504–36515, conference Name: IEEE Access.
67. Mattsson, L.-G. and E. Jenelius, Vulnerability and resilience of transport systems – A discussion of recent research. *Transportation Research Part A: Policy and Practice*, Vol. 81, 2015, pp. 16–34.
68. Manso, G., B. Balsmeier, and L. Fleming, Heterogeneous Innovation and the Antifragile Economy, 2020.
69. Ramezani, J. and L. M. Camarinha-Matos, Approaches for resilience and antifragility in collaborative business ecosystems. *Technological Forecasting and Social Change*, Vol. 151, 2020, p. 119846.
70. Kim, H., S. Muñoz, P. Osuna, and C. Gershenson, Antifragility Predicts the Robustness and Evolvability of Biological Networks through Multi-Class Classification with a Convolutional Neural Network. *Entropy*, Vol. 22, No. 9, 2020, p. 986, number: 9 Publisher: Multidisciplinary Digital Publishing Institute.
71. Axenie, C., D. Kurz, and M. Saveriano, Antifragile Control Systems: The Case of an Anti-Symmetric Network Model of the Tumor-Immune-Drug Interactions. *Symmetry*, Vol. 14, No. 10, 2022, p. 2034, number: 10 Publisher: Multidisciplinary Digital Publishing Institute.
72. Axenie, C. and M. Saveriano, *Antifragile Control Systems: The case of mobile robot trajectory tracking in the presence of uncertainty*, 2023, arXiv:2302.05117 [cs, eess].

73. Fang, Y. and G. Sansavini, Emergence of Antifragility by Optimum Postdisruption Restoration Planning of Infrastructure Networks. *Journal of Infrastructure Systems*, Vol. 23, No. 4, 2017, p. 04017024, publisher: American Society of Civil Engineers.
74. Cobianchi, L., F. Dal Mas, A. Peloso, L. Pugliese, M. Massaro, C. Bagnoli, and P. Angelos, Planning the Full Recovery Phase. *Annals of Surgery*, Vol. 272, No. 6, 2020, pp. e296–e299.
75. Priyadarshini, J., R. K. Singh, R. Mishra, and S. Bag, Investigating the interaction of factors for implementing additive manufacturing to build an antifragile supply chain: TISM-MICMAC approach. *Operations Management Research*, Vol. 15, No. 1, 2022, pp. 567–588.
76. de Bruijn, H., A. Größler, and N. Videira, Antifragility as a design criterion for modelling dynamic systems. *Systems Research and Behavioral Science*, Vol. 37, No. 1, 2020, pp. 23–37, _eprint: https://onlinelibrary.wiley.com/doi/pdf/10.1002/sres.2574.
77. Taleb, N. N. and J. West, Working with Convex Responses: Antifragility from Finance to Oncology. *Entropy*, Vol. 25, No. 2, 2023, p. 343, number: 2 Publisher: Multidisciplinary Digital Publishing Institute.
78. Tan, W. J., A. N. Zhang, and W. Cai, A graph-based model to measure structural redundancy for supply chain resilience. *International Journal of Production Research*, Vol. 57, No. 20, 2019, pp. 6385–6404, publisher: Taylor & Francis _eprint: https://doi.org/10.1080/00207543.2019.1566666.
79. Kamalahmadi, M., M. Shekarian, and M. Mellat Parast, The impact of flexibility and redundancy on improving supply chain resilience to disruptions. *International Journal of Production Research*, Vol. 60, No. 6, 2022, pp. 1992–2020, publisher: Taylor & Francis _eprint: https://doi.org/10.1080/00207543.2021.1883759.
80. Johnson, J. and A. V. Gheorghe, Antifragility analysis and measurement framework for systems of systems. *International Journal of Disaster Risk Science*, Vol. 4, No. 4, 2013, pp. 159–168.
81. Munoz, A., J. Billsberry, and V. Ambrosini, Resilience, robustness, and antifragility: Towards an appreciation of distinct organizational responses to adversity. *International Journal of Management Reviews*, Vol. 24, No. 2, 2022, pp. 181–187, _eprint: https://onlinelibrary.wiley.com/doi/pdf/10.1111/ijmr.12289.
82. Qin, S. J. and T. A. Badgwell, A survey of industrial model predictive control technology. *Control engineering practice*, Vol. 11, No. 7, 2003, pp. 733–764.
83. Darby, M. L. and M. Nikolaou, MPC: Current practice and challenges. *Control Engineering Practice*, Vol. 20, No. 4, 2012, pp. 328–342.
84. Lucia, S., A. Tătulea-Codrean, C. Schoppmeyer, and S. Engell, Rapid development of modular and sustainable nonlinear model predictive control solutions. *Control Engineering Practice*, Vol. 60, 2017, pp. 51–62.
85. Andersson, J. A. E., J. Gillis, G. Horn, J. B. Rawlings, and M. Diehl, CasADi – A software framework for nonlinear optimization and optimal control. *Mathematical Programming Computation*, Vol. 11, No. 1, 2019, pp. 1–36.
86. Wächter, A. and L. T. Biegler, On the implementation of an interior-point filter line-search algorithm for large-scale nonlinear programming. *Mathematical Programming*, Vol. 106, No. 1, 2006, pp. 25–57.

87. Vlahogianni, E. I., M. G. Karlaftis, and J. C. Golias, Short-term traffic forecasting: Where we are and where we're going. *Transportation Research Part C: Emerging Technologies*, Vol. 43, 2014, pp. 3–19.
88. Lana, I., J. Del Ser, M. Velez, and E. I. Vlahogianni, Road Traffic Forecasting: Recent Advances and New Challenges. *IEEE Intelligent Transportation Systems Magazine*, Vol. 10, No. 2, 2018, pp. 93–109, conference Name: IEEE Intelligent Transportation Systems Magazine.
89. Lillicrap, T. P., J. J. Hunt, A. Pritzel, N. Heess, T. Erez, Y. Tassa, D. Silver, and D. Wierstra, *Continuous control with deep reinforcement learning*, 2015, arXiv:1509.02971.
90. Mnih, V., K. Kavukcuoglu, D. Silver, A. Graves, I. Antonoglou, D. Wierstra, and M. Riedmiller, Playing Atari with Deep Reinforcement Learning, 2013.
91. Zhang, S., H. Yao, and S. Whiteson, Breaking the Deadly Triad with a Target Network. In *Proceedings of the 38th International Conference on Machine Learning*, PMLR, 2021, pp. 12621–12631, iSSN: 2640-3498.
92. Silver, D., G. Lever, N. Heess, T. Degris, D. Wierstra, and M. Riedmiller, Deterministic Policy Gradient Algorithms, 2014.
93. Mazloumi, E., G. Currie, and G. Rose, Using GPS Data to Gain Insight into Public Transport Travel Time Variability. *Journal of Transportation Engineering*, Vol. 136, No. 7, 2010, pp. 623–631.